Characterizing Phase-Only fMRI Data with an Angular Regression Model

Christopher P. Meller[1] and Daniel B. Rowe[2,3]
[1]Division of Biostatistics, [2]Department of Biophysics, [3]Corresponding Author
Medical College of Wisconsin, 8701 Watertown Plank Road, Milwaukee, WI 53226

Abstract:

It is well known that fMRI voxel time series are complex-valued with real and imaginary parts. The complex-valued voxel time series are transformed from real-imaginary rectangular coordinates to equivalent information magnitude-phase polar coordinates. Magnitude-only data models that discard the phase portion of the data have dominated fMRI analysis. However these analyzes discard half of the data which may contain valuable biologic information about the vasculature. When phase-only time series defined within plus and minus pi that discard the magnitude portion of the data have been analyzed, ordinary least squares regression has been the technique of choice. We have explored an angular regression alternative to the OLS model which will account for the angular response of the phase. We found an improvement in parameter estimation along with modeling for the angular regression method in experimentally acquired data. Finally, we look at a map of statistics relating association of the observed voxel phase time courses with a reference function in our acquired data and show the possible detection of biological information in the generally discarded phase.

1. Introduction

Functional magnetic resonance imaging (fMRI) is an invaluable tool used to investigate biological phenomena in both animals and humans. However, the results derived from fMRI crucially depend on the model used to analyze the data. It is well known that voxel time courses are complex-valued (Haacke et al., 1999). Traditionally the real-imaginary voxel measurements are converted to informationally equivalent magnitude-phase measurements and the phase portion of the data is discarded. Then, only the magnitude portion of the data is analyzed for experimental or task related changes (Bandettini et al., 1993; Rowe and Logan, 2005). More recently, models that determine task related magnitude changes within the complex-valued data have shown improvements over those that examine magnitude-only data (Rowe and Logan, 2004; Rowe, 2005). However, the just mentioned methods look for magnitude activations whether they be in magnitude-only data or in complex data. There is evidence that the phase portion of the data contains biological information not contained in the magnitude portion of the data indicative of vascularization (Menon, 2002; Nencka and Rowe, 2005) or of possible direct detection of neuronal firing (Borduka et al., 1999).

When modeling either magnitude-only or phase-only data, an ordinary least squares (OLS) regression model is the current analysis standard. We aim to improve modeling of the generally discarded phase portion of the data by using a more appropriate model than OLS. Specifically, we will implement an angular regression model developed by Fisher and Lee (1992) along with the standard OLS model on both simulated and actual experimental fMRI time series data. We will lay the framework for making inferences about possible experimental task related phase changes. In doing this we will have accounted for the angular nature of the response and provided an improvement in dealing with the phase-wrap around issue. In the past the only way to account for phase-wrap in the data was to artifically unwrap it and proceed with an OLS analysis.

2. Background

As previously mentioned, the functional model of the brain and distributional specifications are essential for fMRI analysis results. It is well established that the real and imaginary parts of the complex-valued voxel observations are normally distributed (Gudbjartsson and Patz, 1995; Haacke et al., 1999) provided the dominant noise is scanner related.

2.1 Real-Imaginary Data

The real and imaginary components (y_R, y_I) of the complex-valued data in a voxel at a particular time point have been described as

$$\begin{aligned} y_R &= \rho\cos\theta + \eta_R \\ y_I &= \rho\sin\theta + \eta_I \end{aligned} \tag{2.1}$$

where (ρ, θ) are the magnitude and phase from a conversion to polar coordinates and (η_R, η_I) are the

real and imaginary noise components (Rowe and Logan, 2004). Additionally, the real and imaginary noise has been well characterized by a normal distribution with mean zero and covariance matrix Σ denoted $(\eta_R, \eta_I)' \sim N(0, \Sigma)$ where $\Sigma = \sigma^2 I_2$. The joint distribution of $(y_R, y_I)'$ is bivariate normal with mean $(\rho\cos\theta, \rho\sin\theta)'$ and covariance matrix Σ. The above description is for a single time point and a t subscript for temporally ordered observations will be omitted until specifically noted.

2.2 Magnitude-Phase Data

The above mentioned complex-valued data is commonly transformed into magnitude and phase polar coordinates $r = \sqrt{y_R^2 + y_I^2}$ and $\phi = \tan^{-1}(y_I/y_R)$ with Jacobian r. It is important to understand that the previous distributional specifications were on the observed real and imaginary parts of the data and not on the magnitude or phase that the data are transformed to. The derivation of the joint distribution of r and ϕ is presented in Rowe and Logan (2004) and has the form

$$p(r,\phi) = \frac{r}{2\pi\sigma^2} e^{-\frac{1}{2\sigma^2}\left[r^2+\rho^2-2\rho r\cos(\phi-\theta)\right]} \quad (2.2)$$

where $r, \rho, \sigma > 0$ and $-\pi < \phi, \theta \leq \pi$.

2.3 Magnitude-Only Data

The above joint magnitude and phase distribution is then marginalized when considering magnitude-only data. The phase data is integrated out or discarded and the resulting magnitude distribution is Ricean and given by

$$p(r) = \frac{r}{\sigma^2} e^{-\frac{r^2+\rho^2}{2\sigma^2}} \int_0^{2\pi} e^{-\frac{r\rho}{\sigma^2}\cos(\alpha)} d\alpha \quad (2.3)$$

where $r, \rho, \sigma > 0$. The integral term is generally denoted by $I_0(r\rho/\sigma^2)$, a zeroth order modified Bessel function of the first kind. If we define signal-to-noise ratio (SNR) to be ρ/σ we see that the magnitude is Rayleigh distributed for SNR=0. If the SNR is "large," say greater than 10, then the Ricean distribution approaches the normal distribution

$$p(r) = (2\pi\sigma^2)^{-1/2} e^{-\frac{(r-\rho)^2}{2\sigma^2}} \quad (2.4)$$

with population mean magnitude ρ and variance σ^2 where $r, \rho, \sigma > 0$. There has been interest in determining SNR cut-off values in which the Rayleigh and normal distributional approximations hold (Rowe, 2005). But even if these cut-off values are known the voxel-wise SNR is not known *a priori* and may fall within them. An alternative approximation to the Ricean distribution valid for any SNR has been explored (Rowe, 2005) that utilizes a Taylor series expansion for the cosine in the exponent of the integral term.

2.4 Phase-Only Data

Similar to the magnitude-only case, the marginal distribution for the phase can be derived to be

$$p(\phi) = \frac{e^{-\frac{\rho^2}{2\sigma^2}}}{2\pi}\left[1 + \frac{\rho}{\sigma}\sqrt{2\pi}\cos(\phi-\theta_0) e^{\frac{\rho^2\cos^2(\phi-\theta_0)}{2\sigma^2}} \times \int_{z=-\infty}^{\frac{\rho\cos(\phi-\theta_0)}{\sigma}} \frac{e^{-z^2/2}}{\sqrt{2\pi}} dz\right] \quad (2.5)$$

where $-\pi < \phi, \theta \leq \pi$ and $\rho, \sigma > 0$. Parallel with the magnitude, the marginal distribution of the phase approaches the normal distribution

$$p(\phi) = [2\pi(\sigma/\rho)^2]^{-1/2} e^{-\frac{(\phi-\theta)^2}{2(\sigma/\rho)^2}} \quad (2.6)$$

with mean θ and variance $(\sigma/\rho)^2$ for large SNR. Although OLS can be applied to any set of data without a distributional specification, this limiting distribution allows not only OLS to be used to fit a model to this data but also hypotheses to be tested. However, phase data lies within an interval of $(-\pi, \pi]$ which leaves it vulnerable to phase-wrap and can cause the OLS model fit to be questionable as will be shown later. We define phase-wrap to be the event of successive phase measurement points crossing a $|\pi|$ boundary. Phase-wrap is detected by differencing pairs of temporally adjacent phase values and defining a phase-wrap when the difference is greater than $|\pi|$.

Introducing the subscript, t, for each time point combined with the limiting distribution we are able to model the phase

$$\phi_t = \tan^{-1}\left[\frac{\rho_t\sin(\theta_t) + \eta_{It}}{\rho_t\cos(\theta_t) + \eta_{Rt}}\right], \quad t = 1, \ldots, n, \quad (2.7)$$

with a normal distribution and an OLS model. One can see that the argument of the four quadrant inverse tangent is the ratio of noncentral normal variates. The ratio of noncentral normal variates has been studied by Marsaglia (1965) who showed that it can be symmetric, asymmetric, unimodal or bimodal.

3. Models

As previously noted, phase-only time series data is rarely analyzed in fMRI, because it is sensitive to physiologic noise. It has been argued that respiration causes movement of internal organs which in

turn alters the B-field and thus the phase. When fMRI phase time seried data is analyzed, the OLS model is utilized (Borduka et al., 1999). Before an OLS model can be fit, the time series needs to be artificially unwrapped. The process of artificially unwrapping the data and then fitting an OLS model to it will be described shortly. Menon (2002) looked at phase time series after unwrapping and noticed an approximate linear correlation with the magnitude data which he believed was attributed to large blood vessels. The OLS model will be briefly summarized then an alternative model will be introduced along with its advantages and disadvantages.

3.1 Ordinary Least Squares Regression

The OLS phase-only data model at time t for an arbitrary voxel can be written as

$$\phi_t = u_t'\gamma + \delta_t, \tag{3.1}$$

where ϕ_t is the observed phase angle measurements, u_t' is a specific row of a design matrix U, an example of which is presented in Eqn. 3.2, γ are the fixed but unknown phase regression coefficients, and δ_t is the measurement error. This measurement error is assumed to originate from the normal distribution $N(0, \tau_t^2)$ where $\tau_t^2 = \sigma^2/\rho_t^2$. For our example that will be presented later $U = (u_1, ..., u_n)'$ is constructed to have three covariates,

$$U = \begin{pmatrix} 1 & 1 & 1 \\ 1 & 2 & 1 \\ \vdots & \vdots & \vdots \\ 1 & 17 & -1 \\ \vdots & \vdots & \vdots \\ 1 & 256 & -1 \end{pmatrix}. \tag{3.2}$$

The above design matrix includes a column of 1's to model the intercept, a column of counting numbers to account for a possible linear trend over time, and a third column with alternating sets of 16 1's and -1's to characterize a task related reference function. Sets of 16 are used in our matrix to coincide with both our simulated and acquired experimental data which have stimulus lengths of 16 observations.

The SNR at time t is defined to be $\rho_t/\sigma = (\beta_0 + \beta_1 t + \beta_2 u_{2t})/\sigma$ but $\beta_1 t + \beta_2 u_{2t}$ is generally very small when compared to β_0 within the brain and zero outside the brain. The approximation $\rho_t/\sigma \approx \beta_0/\sigma$ is utilized and the variance in a given voxel becomes constant over time. When the phase-only data is described with the large SNR OLS model, hypotheses can be tested using a $d \times (q+1)$ phase contrast matrix D where d is the number of constraints or rows of D and q is the number of non baseline regressors. Inferences can be drawn using standard linear contrast tests H_0: $D\gamma = 0$ vs H_1: $D\gamma \neq 0$. This testing procedure leads to the unrestricted, $(\hat{\gamma}, \hat{\tau}^2)$, and restricted, $(\tilde{\gamma}, \tilde{\tau}^2)$, maximum likelihood estimates for γ and τ^2 having the usual form. Then the generalized likelihood ratio statistic $-2\log\lambda$ for testing task related phase changes is formed. This statistic has a large sample χ^2 distribution with d degrees of freedom which is the difference in the number of constraints between the alternative and null hypotheses. The degrees of freedom d is also equal to the full row rank of D. We also may simplify the large sample χ^2 statistic using algebra to arrive at an exact F statistic or t statistic provided $d = 1$.

The angular response of the phase-only OLS model can cause modeling problems at the phase-wrap junction if not accounted for properly, thus resulting in poor parameter estimation and incorrect inferences. When a combination of the three following conditions are valid we can describe the phase data with little concern using our standard OLS regression model. These conditions are 1) a large SNR, 2) our baseline angle, γ_0, is not near either the upper boundary of π or the lower boundary of $-\pi$, and 3) the linear trend is small enough that the data does not rise or fall beyond π and $-\pi$. The large SNR assumption makes the probability of a large difference between successive measurements very small.

However, in real acquired experimental fMRI data the SNR and mean phase in voxels varies greatly over space. The above stringent conditions are, in general, not met across an image. Often within an fMRI data set phase angles are observed close to $\pm\pi$. As previously mentioned, the method generally used to deal with this issue is "unwrapping." Unwrapping is the process of beginning with the first observation, proceeding through the time series and flagging an observation in which the next point in the time series has an absolute difference greater than or equal to a predefined value, generally π, then shifting the rest of the time series by $\pm 2\pi$. This process is repeated to the end of the time series. However, when the assumption of high SNR becomes suspect, the model fails and the investigator needs another model.

In many instances there is no phase-wrap and simply fitting an OLS regression line to the data is sufficient. We implement an angular model procedure to deal with the angular nature of the response will allow us to relax the large SNR requirement.

3.2 Linear-Circular Regression

Fitting an OLS regression model to artificially unwrapped data may not be an ideal method and is especially poor for low and moderate SNR data. We adopt the angular regression model by Fisher and Lee (1992) for fMRI phase data.

The von Mises distribution, also known as the circular normal distribution is the underlying distribution in angular models (Jammalamadaka and SenGupta, 2001). This distribution specifically deals with random variables on the interval of $(-\pi, \pi]$. The general von Mises distribution is the conditional distribution of the phase given the magnitude. The von Mises distribution is found by dividing the joint distribution $p(\phi, r)$ in Eqn. 2.2 by the marginal $p(r)$ in Eqn. 2.3 as

$$p(\phi|r) = \frac{e^{\kappa \cos(\phi-\theta)}}{2\pi I_0(\kappa)} \quad (3.3)$$

where $\kappa = r\rho/\sigma^2$, $-\pi \leq \phi, \theta < \pi$, and $0 \leq \kappa < \infty$. This derived conditional distribution is referred to as a von Mises with mean θ and concentration κ (Jammalamadaka and SenGupta, 2001). Again $I_0(\cdot)$ is the zeroth order modified Bessel function of the first kind. The von Mises distribution has a limiting normal distribution with mean θ and variance $1/\kappa$ when κ is large. The linear-circular regression models utilize the von Mises distribution conditional upon the population and sample magnitudes being unity.

We adopt the model by Fisher and Lee (1992) that allows for multiple predictor variables and relaxes the need for distributional assumptions on the design matrix. Their model assumes the angular observations $\phi_1, \ldots, \phi_n$ are temporally independent von Mises distributed with constant concentration parameter κ. Each ϕ_t originates from a von Mises distribution with mean θ_t and concentration κ. The fixed concentration parameter model is

$$\theta_t = \gamma_0 + g(w_t'\gamma) \quad (3.4)$$

where the design matrix W with the t^{th} row $w_t' = (w_{1t}, \ldots, w_{(q+1)t})$ is comprised of all columns except the first in the design matrix U as defined in the previous section. Of course, W can include additional covariates, but we will focus on our particular choice. There is no need to include the baseline column in W, because the intercept is already estimated within the model. The link function $g(\cdot)$ has the purpose of mapping its argument to be in $-\pi$ to π. The use of a link function eliminates the non-identifiability problem of MLEs that is present in the Gould model. One possible link function that given by Fisher and Lee that we will use is

$$g(\cdot) = 2\tan^{-1}\left(\text{sgn}(\cdot)\,|\cdot|^{\nu}\right) \quad (3.5)$$

where $\text{sgn}(\cdot)$ is the operator that returns the sign of its argument, $\tan^{-1}(\cdot)$ is a two quadrant inverse tangent, and the transformation parameter ν can be estimated from the data similar to the Box-Cox transformation (Box and Cox, 1964; Fisher and Lee, 1992).

Fisher and Lee give us equations to obtain parameter estimates and draw inferences using the model in Eq. 3.4 with the link function given in Eq. 3.5, where $\nu = 1$. Of course, the link function can be chosen differently, but we will illustrate fitting the Fisher and Lee model with this particular choice. First, we define the natural log likelihood, denoted $\log L$

$$\begin{aligned} \log L &= -n\log 2\pi - n\log I_0(\kappa) \\ &\quad +\kappa\sum_{t=1}^{n}\cos(\phi_t - \gamma_0 - g(w_t'\gamma)). \end{aligned} \quad (3.6)$$

Second, the authors define the following

$$\begin{aligned} v_t &= \sin(\phi_t - \gamma_0 - g(w_t'\gamma)), \\ v &= (v_1, \ldots, v_n)', \\ W &= (w_1, \ldots, w_n)' \\ G &= \text{diag}(g'(w_1'\gamma), \ldots, g'(w_n'\gamma)) \\ S &= \frac{1}{n}\sum_{t=1}^{n}\sin(\phi_t - g(w_t'\gamma)) \\ C &= \frac{1}{n}\sum_{t=1}^{n}\cos(\phi_t - g(w_t'\gamma)) \\ R &= (S^2 + C^2)^{1/2}. \end{aligned}$$

In the above v is an $n \times 1$ vector and G is a $n \times n$ matrix while S, C, and R are scalars. The function $g'(\cdot)$ is defined to be the derivative of the link function which in our example is $g'(w_t'\gamma) = 2/[1 + (w_t'\gamma)^2]$. The MLEs are found by solving the following equations

$$\begin{aligned} W'Gv &= 0, \\ \tan(\hat{\gamma}_0) &= S/C, \\ A(\hat{\kappa}) &= R \end{aligned}$$

where $A(\hat{\kappa}) = I_1(\hat{\kappa})/I_0(\hat{\kappa})$. The second equation above involving the four quadrant tangent of $\hat{\gamma}_0$ is found by utilizing the trigonometric addition formula for $\gamma_0 - (\phi_t - g(w_t'\gamma))$ in the log likelihood before differentiation. We begin with an initial value for $\hat{\gamma}$ and calculate values for S, C, and R from the above

equations. An updated value of $\hat{\gamma}$, denoted by $\hat{\gamma}^*$ is then found by solving the following equation for $\hat{\gamma}^*$,

$$(W'G^2W)(\hat{\gamma}^* - \hat{\gamma}) \quad = \quad W'G^2y \qquad (3.7)$$

where $y = (y_1, \ldots, y_n)'$ and $y_t = v_t / [A(\hat{\kappa})g'(w_t'\hat{\gamma})]$. We also find an updated estimate for γ_0 at each iteration by computing $\hat{\gamma}_0$ from the four quadrant inverse tangent $\tan^{-1}(S/C)$ and κ from $A(\kappa)$. The updated estimate of $\hat{\gamma}^*$ is recursively placed back into formulas for a set number of iterations or until the iterative values differ by less than some pre-defined amount. When it is *a priori* known that κ is "large" then the approximation

$$A(\kappa) \quad = \quad \left(1 - \frac{1}{2\kappa} - \frac{1}{8\kappa} - \cdots\right)$$

can be utilized while if it is *a priori* known that κ is "small" then the approximation

$$A(\kappa) \quad = \quad \frac{\kappa}{2}\left(1 - \frac{\kappa^2}{8} + \frac{\kappa^4}{48} - \cdots\right)$$

can be utilized (Jammalamadaka and SenGupta, 2001). When κ is above 1.25, the large κ approximation works well and one can simply approximate $\hat{\kappa}$ by

$$\hat{\kappa} = \frac{1 + \sqrt{3 - 2R}}{4(1 - R)} \qquad (3.8)$$

while if κ is below .75, then one can simply approximate $\hat{\kappa}$ by

$$\hat{\kappa} = 2R\ . \qquad (3.9)$$

for intermediate values, a simple average works well.

Fisher and Lee also give the large sample variance of the estimated coefficient vector,

$$var(\hat{\gamma}) \quad = \quad \frac{1}{\hat{\kappa}A(\hat{\kappa})}\left\{\left(W'G^2W\right)^{-1} + \frac{\left(W'G^2W\right)^{-1}W'gg'W\left(W'G^2W\right)^{-1}}{\left(n - g'W\left(W'G^2W\right)^{-1}W'g\right)}\right\},$$

which allows inferences on our γ's where g is a vector whose elements are the diagonal elements of G. They also describe the large sample variance for $\hat{\gamma}_0$ and $\hat{\kappa}$ to be $[(n-q)\hat{\kappa}A(\hat{\kappa})]^{\frac{1}{2}}$ and $1/(nA'(\hat{k}))$, respectively, where $A'(\kappa) = 1 - A(\kappa)/\kappa - A^2(\kappa)$ is the derivative of the ratio of the Bessel functions with respect to κ. The variance of the large sample normal limiting distribution of the von Mises is $1/\kappa$ (Jammalamadaka and SenGupta, 2001).

The fitted phase time course can then be plotted to compare to the observed time course utilizing

$$\hat{\phi}_t = \tan^{-1}\left[\frac{\sin(\hat{\gamma}_0 + g(w_t'\hat{\gamma}))}{\cos(\hat{\gamma}_0 + g(w_t'\hat{\gamma}))}\right]$$

because, although $g(\cdot)$ is within $-\pi$ to π, the addition of $\hat{\gamma}_0$ may shift it out of this interval. We can then use a normal approximation to test the hypothesis, H_0: $\gamma_m = 0$ verses H_1: $\gamma_m \neq 0$ using the constructed test statistics, $\hat{\gamma}_m/\sqrt{var(\hat{\gamma}_m)}$. Alternatively, one could set up linear contrast hypothesis tests and obtain the likelihood ratio statistic $-2\log\lambda$, then use the large sample χ^2_d distribution to draw inferences.

4. Experimental Data

A bilateral sequential finger tapping experiment was performed in a block design with 16s off followed by eight epochs of 16s on and 16s off. Scanning was performed using a 1.5T GE Signa in which 5 axial slices of size 96×96 were acquired with a gradient echo pulse sequence having a $FA = 90^\circ$ and a $TE = 47$ms. In image reconstruction, the acquired data was zero filled to 128×128. After Fourier image reconstruction, each voxel has dimensions in mm of $1.5625 \times 1.5625 \times 5$. Observations were taken every TR= 1000ms so that there are 272 in each voxel. Data from a single axial slice through the sensorimotor cortex was selected for analysis. Pre-processing included the removal of the first three points to omit magnetic field equalization effects followed by the use of an ideal 0/1 frequency filter to remove respiration, scanner drift, and low frequency physiological noise.

Before examining the phase-only data, we looked at the magnitude-only data. An OLS model is fit to the magnitude-only time series in each voxel with design matrix $X = U$ as previously described and magnitude-only regression coefficients $\beta = (\beta_0, \beta_1, \beta_2)'$. We computed activation t-statistics in each voxel testing the hypothesis of the coefficient corresponding to the reference function in the last column of X being zero. The bilateral activation in the motor cortex regions for the magnitude-only OLS model can be seen in Fig. 1a along with the activation along the midline in the supplemental motor area. In Fig. 1a are t-statistics with a threshold that was Bonferroni corrected for multiple comparisons, as described in Logan and Rowe (2004), at a 5% family wise error (FWE) rate.

If the phase-only data contains no information regarding possible biological phenomena in the brain we would anticipate seemingly random activations above the threshold. If the phase-only data is to contain information regarding possible biological phenomena in the brain we would anticipate seeing phase activations with some sort of pattern. One possible pattern is to be in similar locations as the

magnitude-only activations. The association between magnitude-only and phase-only time series observed by Menon for areas with large blood vessels would suggest phase activations can be found in similar places as magnitude activations, given that such blood vessels are present (Menon, 2002; Nencka and Rowe, 2005). Any similarities between the statistics for the magnitude-only and phase-only models would strengthen the idea that valuable temporal phase information is discarded when magnitude-only data is analyzed.

Although as seen in Fig. 1 b-d the three models produce similar thresholded phase-only activation maps with focal positively associated voxel time series within the primary motor cortex which is where the difuse magnitude-only activations were found. Even though the three phase-only models produce similar activation maps, the parameter estimates are radically different. As seen in Fig. 2a-c, the estimated baseline phase angles, the γ_0's are similar within the brain for the OLS model in Fig. 2a, the unwrapped OLS model in Fig. 2b, and the Fisher-Lee model in Fig. 2c, except for about a dozen voxels with the OLS model along two vertical waivey lines bordering a baseline $\pm\pi$ transition, but are all very diferent outside the brain. In Fig. 2d-f, the linear trend coefficients, the γ_1's are similar within the brain for the OLS model in Fig. 2d, the unwrapped OLS model in Fig. 2e, and the Fisher-Lee model in Fig. 2f, except for a few dozen voxels with the OLS model along two waivey lines of obviously different values which are along a baseline $\pm\pi$ transition, but are all very diferent outside the brain. In Fig. 2g-i, the reference function coefficients, the γ_2's are similar within the brain for the OLS model in Fig. 2g, the unwrapped OLS model in Fig. 2h, and the Fisher-Lee model in Fig. 2i, except for a few dozen voxels with the OLS model along two waivey lines of obviously different values which are along a baseline $\pm\pi$ transition, but are very diferent outside the brain. In Fig. 2j-l the variance estimates, the σ_2's are similar within the brain for the OLS model in Fig. 2j, the unwrapped OLS model in Fig. 2k, and the Fisher-Lee model in Fig. 2l, except for a few dozen voxels with the OLS model along two waivey lines of obviously different values which are along a baseline $\pm\pi$ transition, but are very diferent outside the brain. Further note that the variance estimate for many voxels is lower with the Fisher-Lee model as compared to the other two models.

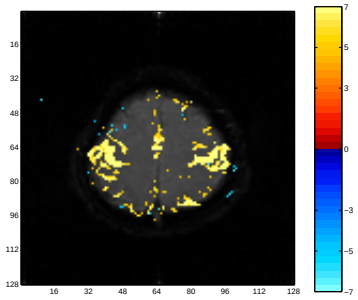

(a) OLS Magnitude-only

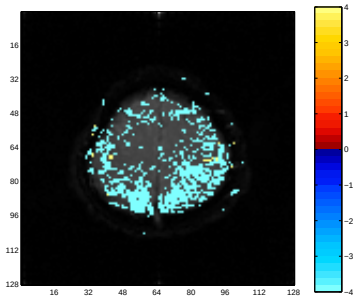

(b) OLS Phase-only

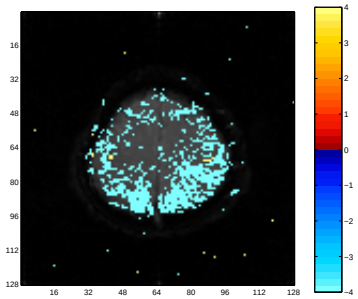

(c) UNW Phase-only

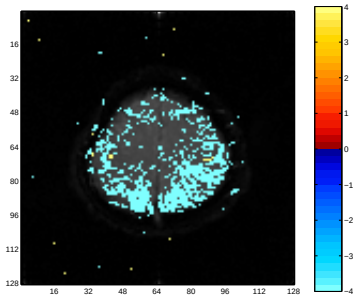

(d) FL Phase-only

Figure 1: Phase-only thresholded activations.

We fit each time series with two OLS regressions (with and without unwrapping) and the Fisher-Lee angular regression, then compared the results. The OLS models fit the data poorly as seen by their estimated parameter values even though the phase activation statistics are similar. The unwrapped OLS model performs similarly to the OLS model within the brain with some false positives outside the brain. Outside the brain the OLS model without unwrapping the data does not pick up false positives. The Fisher-Lee model performs similarly within the brain to the OLS models and also outside the brain with about the same small number of false positives as with the unwrapped OLS model.

5. Conclusion

Modeling fMRI phase time series with OLS regression results in some troublesome phenomena, which include poor fit, incorrect parameter estimation, and potentially inaccurate test statistics, even after being unwrappped. Most of these problem arise from the issue of phase-wrap in the time series. We implemented a model by Fisher and Lee (1992). It allowed us to define a design matrix which could account for several regressors including a linear trend and a reference function from which to make and test hypothesis using a large sample asymptotic z statistic.

The actual phase time series we presented solidified our findings that the Fisher-Lee model is an excellent choice for fitting with fMRI phase-only data. We showed a specific voxel example where OLS was unable to match the modeling accuracy of the Fisher-Lee model and actually contained fitted values not consistent with the fMRI phase angular property. Fisher and Lee's model is less suseptible to low SNR problems, and if applied to other real data examples with more noise, we would expect it to perform as well as OLS. In real fMRI data that is of a higher resolution with smaller voxels, we expect there to be a larger difference between the two models. This newly implemented angular model does detect temporal correlations between the phase time course and a reference function in many of the same places as the OLS models.

References

[1] P.A. Bandettini, A. Jesmanowicz, E.C. Wong, and J.S. Hyde. Processing strategies for time-course data sets in functional MRI of the human brain. *Magn. Reson. Med.*, 30(2):161–173, 1993.

[2] J. Borduka, A. Jesmanowicz, J.S. Hyde, H. Xu, Estkowski L., and S.-J. Li. Current-induced magnetic resonance phase imaging. *J. of Magn. Reson.*, 137:265–271, 1999.

[3] G.E.P. Box and D.R. Cox. An analysis of transformations. *J. Roy. Stat. Soc.*, 26:296–311, 1964.

[4] N.I. Fisher and A.J. Lee. Regression models for an angular response. *Biometrics*, 48:665–677, 1992.

[5] H. Gudbjartsson and S. Patz. The Rician distribution of noisy data. *Magn. Reson. Med.*, 34(6):910–914, 1995.

[6] E.M. Haacke, R. Brown, M. Thompson, and R. Venkatesan. *Magnetic Resonance Imaging: Principles and Sequence Design*. John Wiley and Sons, New York, NY, USA, 1999.

[7] S.R. Jammalamadaka and A. SenGupta. *Topics in Circular Statistics*. World Scientific Publishing Co., Singapore, 2001.

[8] B.R. Logan and D.B. Rowe. An evaluation of thresholding techniques in fMRI analysis. *NeuroImage*, 22(1):95–108, 2004.

[9] G. Marsaglia. Ratios of normal variables and ratios of sums of uniform variables. *J. Am. Stat. Assoc.*, 60:193–204, 1965.

[10] R.S. Menon. Postacquisition suppression of large-vessel BOLD signals in high-resolution fMRI. *Magn. Reson. Med.*, 47(1):1–9, 2002.

[11] A.S. Nencka and D.B. Rowe. Complex constant phase activation model removes venous bold contribution in fMRI. *Proc. Soc. of Magn. Reson. Med.*, 13:495, 2005.

[12] D.B. Rowe. *Multivariate Bayesian Statistics*. Chapman & Hall/CRC Press, Boca Raton, FL, USA, 2003.

[13] D.B. Rowe. Parameter estimation in the magnitude-only and complex-valued fMRI data models. *NeuroImage*, 25(4):1124–1132, 2005.

[14] D.B. Rowe and B.R. Logan. A complex way to compute fMRI activation. *NeuroImage*, 23(3):1078–1092, 2004.

[15] D.B. Rowe and B.R. Logan. Complex fMRI analysis with unrestricted phase is equivalent to a magnitude-only model. *NeuroImage*, 24(2):603–606, 2005.

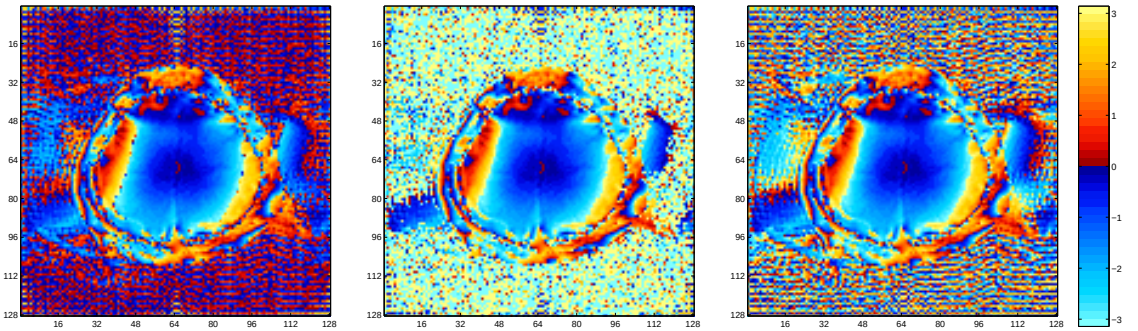

(a) OLS: γ_0 (b) UNW: γ_0 (c) FL: γ_0

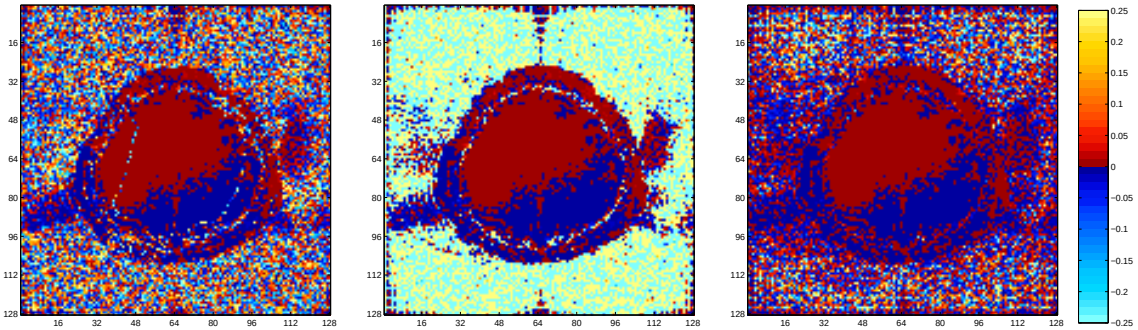

(d) OLS: γ_1 (e) UNW: γ_1 (f) FL: γ_1

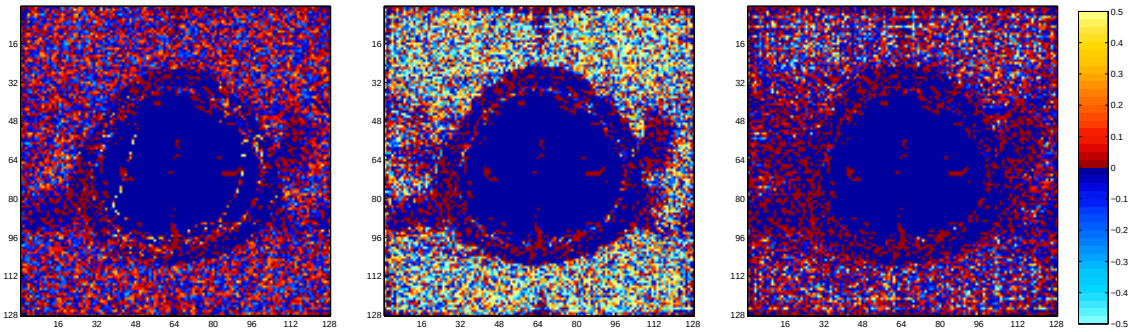

(g) OLS: γ_2 (h) UNW: γ_2 (i) FL: γ_2

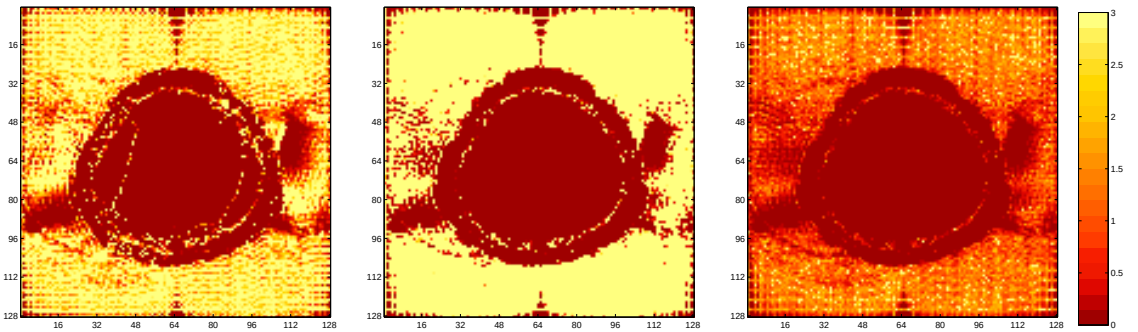

(j) OLS: σ^2 (k) UNW: σ^2 (l) FL: σ^2

Figure 2: Estimated parameters for the three models.